Corp., Madison, WI): P3 (data collection), SHEXTL (version 5.1; structure solution and refinement).

X-ray Crystal Structure of (*Z*)-10d. Suitable crystals were obtained by slow vapor diffusion of ether into a THF solution of (*Z*)-**10d**. The resulting orange prisms were mounted on fine glass fibers with epoxy cement, and X-ray data were collected as summarized in Table II. Crystal symmetry and unit cell parameters were determined as above from 15 centered reflections ($20° \leq 2\theta \leq 25°$). Data were corrected for *Lp* effects and for absorption based upon a series of Ψ scans. The general techniques employed have been previously described.[54]

The position of the rhenium was obtained from a three-dimensional Patterson map. Several least-squares refinements, followed by a difference Fourier synthesis, yielded all non-hydrogen atoms. All non-hydrogen atoms were refined with anisotropic temperature factors. All hydrogens were assigned and held in their calculated positions (d(C-H) = 0.95 Å).[55] Software: P$\bar{1}$ (data collection), modified SHELX-76 (data reduction and refinement).

MO Calculations. Extended Hückel calculations[56] were conducted with weighted H_{ij} formula. The rhenium and phosphorus atoms of the model compounds were assigned idealized octahedral and tetrahedral geometries, respectively. The C=C carbons were assigned idealized trigonal-planar geometries. The Re—C_α, C=C, C—H, C—O, and O—H bonds were assigned lengths of 2.10, 1.32, 1.09, 1.43, and 0.98 Å, respectively. The remaining bond lengths and H_{ij} and ζ parameters used were the same as reported previously.[13a,d,42a]

Acknowledgment. We thank the NIH for support of this research and A. Patton for help with the X-ray data. The NMR spectrometers utilized were acquired via NSF, DOD, and NIH instrumentation grants, and the diffractometer used (University of Delaware) was obtained via an NSF instrumentation grant.

Supplementary Material Available: Additional NOE data and tables of bond distances and angles, hydrogen atom coordinates, and anisotropic and isotropic thermal parameters for (*E*)-**2d** and (*Z*)-**10d** (10 pages); listing of observed and calculated structure factors (41 pages). Ordering information is given on any current masthead page.

(54) Churchill, M. R.; Lashewycz, R. A.; Rotella, F. J. *Inorg. Chem.* **1977**, *16*, 265.
(55) Churchill, M. R. *Inorg. Chem.* **1973**, *12*, 1213.
(56) (a) Hoffmann, R. *J. Chem. Phys.* **1963**, *39*, 1397. (b) Hoffmann, R.; Lipscomb, W. N. *Ibid.* **1962**, *36*, 2179 and 3489; **1962**, *37*, 2872.

Synthesis, Photochemistry, and Electrochemistry of (P)Ge(R_2) and (P)Ge(R)X (P = TPP or OEP, R = CH_3, $CH_2C_6H_5$, or C_6H_5, and X = Cl^-, OH^-, or ClO_4^-)

K. M. Kadish,*[1a] Q. Y. Xu,[1a] J.-M. Barbe,[1a,b] J. E. Anderson,[1a] E. Wang,[1a,c] and R. Guilard*[1b]

Contribution from the Department of Chemistry, University of Houston, Houston, Texas 77004, and Laboratoire de Synthèse et d'Electrosynthèse Organométallique, Associé au C.N.R.S., UA 33, Faculté des Sciences "Gabriel", 21100 Dijon, France. *Received April 3, 1987*

Abstract: The synthesis and characterization of (P)Ge(R_2) and (P)Ge(R)X, where P is the dianion of octaethylporphyrin (OEP) or the dianion of tetraphenylporphyrin (TPP), R is CH_3, $CH_2C_6H_5$, or C_6H_5, and X is ClO_4^-, Cl^-, or OH^-, is described. Each complex was characterized by ^1H NMR, IR, and UV-visible spectroscopy and electrochemistry. The investigated (P)Ge(R_2) complexes can be reduced and oxidized by up to two electrons. The reductions are reversible but a rapid cleavage of the germanium-carbon bond follows the initial electrooxidation. The final oxidation product after the abstraction of one electron from (P)Ge(R_2) was identified as (P)Ge(R)X, where X = ClO_4^-, Cl^-, or OH^- depending on the solvent/supporting electrolyte system. (P)Ge(R)Cl could also be generated from (P)Ge(R_2) in solutions of degassed $CHCl_3$ by illumination with visible light. Electrochemical oxidation of (OEP)Ge(C_6H_5)$_2$, (OEP)Ge(C_6H_5)OH, and (OEP)Ge(C_6H_5)Cl gives the same final species which was spectroscopically and electrochemically identified as (OEP)Ge(C_6H_5)ClO_4. Interestingly, (OEP)Ge(C_6H_5)ClO_4 could be converted to (OEP)Ge(C_6H_5)OH by a one-electron electroreduction which was followed by reaction of the generated anion radical with trace H_2O in solution. Finally, an overall scheme for the oxidation and reduction of (P)Ge(R_2) and (P)Ge(R)X porphyrins is presented.

The remarkable antitumor activity of *cis*-dichlorodiammineplatinum(II) (cisplatin)[2] has led to the search for new inorganic anticancer agents. One class of such candidates may include porphyrins and metalloporphyrins. Some porphyrins and metalloporphyrins are powerful photodynamic agents that can render cancer cells vulnerable to light at frequencies that correspond to wavelengths of the porphyrin absorption maxima.[3,4] For example, malignant tumors take up and retain hematoporphyrin to a much greater extent than do normal tissues.[5] The hematoporphyrin then sensitizes these cells so that they are killed by exposure to visible light.

Germanium porphyrins that contain σ-bonded alkyl or aryl ligands are also potential antitumor agents. In this regard, three properties of the alkyl or aryl Ge(IV) complexes are of importance. These are the following: the tendency of tetraphenylporphyrin derivatives to accumulate in malignant tissues,[6] the potential utility of metal alkyls to act as alkylating agents, and the nature of

(1) (a) University of Houston. (b) University of Dijon. (c) On leave from Changchun Institute of Applied Chemistry, Changchun, People's Republic of China.
(2) Prestayko, A. W.; Crooke, S. T.; Carter, S. K. *Cisplatin*; Academic: New York, 1980.
(3) Magnus, I. A. *S. Afr. J. Lab. Clin. Med.* **1963**, *9*, 238.
(4) Mathews-Roth, M. M.; Pathak, M. A.; Fitzpatrick, T. B.; Harber, L. C.; Kass, E. H. *JAMA, J. Am. Med. Assoc.* **1974**, *228*, 1004.
(5) Granelli, S. G.; Diamond, I.; McDonagh, A. F.; Wilson, C. B.; Nielson, S. L. *Cancer Res.* **1975**, *35*, 2567.
(6) Musser, D. M.; Wagner, J. M.; Datta-Grupta, N. *J. Natl. Cancer Inst.* **1978**, *61*, 1397.

0002-7863/87/1509-7705$01.50/0

Table I. Yields and Elemental Analysis for (P)Ge(R)$_2$

compd	recryst solvent[a]	yield (%)	elemental analysis[b] (%) C	H	N
(OEP)Ge(CH_3)$_2$	B	64	71.1 (71.83)	7.9 (7.93)	8.7 (8.82)
(OEP)Ge(C_6H_5)$_2$	C/D 1/1	53	74.4 (75.9)	7.1 (7.17)	7.2 (7.38)
(OEP)Ge($CH_2C_6H_5$)$_2$	B/D 1/1	43	73.5 (76.25)	7.3 (7.42)	7.0 (7.11)
(TPP)Ge(C_6H_5)$_2$	A/D 2/1	60	79.1 (80.12)	4.5 (4.56)	6.6 (6.67)
(TPP)Ge($CH_2C_6H_5$)$_2$	A/D 1/1	51	80.1 (80.29)	4.9 (4.89)	6.3 (6.45)

[a] Solvents: A = toluene, B = benzene, C = 1,2-dichloroethane, D = heptane. [b] Calculated values in parentheses.

elemental germanium to suppress spontaneous mouse tumors.[7]

Miyamoto and co-workers[8] found that rats fed with dimethyl-5,10,15,20-tetrakis[3,5-bis(1,1-dimethylethyl)phenyl]-(porphinato)germanium(IV) at a proper dose had fewer solid tumors than those not fed with this compound. It was also reported that the compound showed considerable activity toward neoplastic tissues both in vitro and in vivo. This suggests that activation of the methyl groups attached to the germanium atom might play a significant role in the anticancer drug action.

Almost 15 years ago, Maskasky and Kenney[9,10] utilized σ-bonded germanium porphyrins as NMR shift reagents. However, since these early reports there have been very few studies on the chemical properties and reactivity of these types of complexes. Pommier and co-workers[11-15] synthesized several (TPP)Ge(R)$_2$ and (OEP)Ge(R)$_2$ compounds that were characterized by UV–visible and ^{1}H NMR spectroscopy. These porphyrins readily reacted with oxygen or light and the apparent photochemical insertion of O_2 into the germanium–carbon bond was compared to similar results for (TPP)Sn(R)$_2$.

Redox processes are most likely to be involved in the antitumor activity of σ-bonded germanium porphyrins, but there have been no detailed electrochemical studies published on these σ-bonded complexes. This is the purpose of the present paper which reports the synthesis, photochemistry, and electrochemistry of dialkyl and diaryl germanium(IV) porphyrins before and after exposure to light in the absence of oxygen.

It is known that alkyl or aryl transition-metal complexes of Fe[16] and cobalt[17,18] can exist in several oxidation states and that the oxidized Co(III) or Fe(III) complex exhibits a reversible electrochemically initiated, metal-to-nitrogen migration of the σ-bonded alkyl or aryl group after electrooxidation. However, σ-bonded alkyl and aryl germanium porphyrin complexes are similar to the non-transition-metal σ-bonded indium[19] and gallium[20] alkyl porphyrins in that the complexes undergo a metal–carbon bond cleavage upon electrochemical oxidation. The product of this electrooxidation is characterized as (P)Ge(R)X, where P = OEP or TPP and X = Cl^-, ClO_4^-, or OH^-, depending upon the solvent and supporting electrolyte. (OEP)Ge(C_6H_5)Cl can also be readily generated under illumination of light in the absence of oxygen. In this present study (P)Ge(R)$_2$ and (P)Ge(R)X were monitored before and after each electrode reaction by electrochemical and spectroelectrochemical techniques as well as by ^{1}H NMR, ESR, and GC techniques. On the basis of these data an overall oxidation/reduction scheme for the mono and bis ligated σ-bonded complexes is presented.

Experimental Section

Instrumentation. Elemental analyses were performed by the Service Central de Microanalyses du CNRS. ^{1}H NMR spectra at 400 MHz were recorded on a Bruker WM 400 spectrometer of the Cerema (Centre de Résonance Magnétique de l'Université de Dijon) or at 300 MHz on a Nicolet NT-300 spectrometer controlled by a Model 293.C programmer. Spectra were measured on 3-mg solutions of complex in $CDCl_3$ with tetramethylsilane as internal reference. IR spectra were obtained on a Perkin-Elmer 580B or a Perkin-Elmer 1330 with samples prepared as 1% dispersion in CsI. Electronic absorption spectra were recorded on either a Perkin-Elmer 559 spectrophotometer, an IBM Model 9430 spectrophotometer, or a Tracor Northern 1710 holographic optical spectrophotometer–multichannel analyzer. The photochemical synthesis was performed under argon with use of a visible OSRAM HQI-400W source.

Cyclic voltammetry at potential scan rates slower than 0.3 V/s was carried out on either a Princeton Applied Research Model 174A potentiostat or an IBM Instruments Model EC 225 voltammetric analyzer. Current voltage curves were recorded on a Houston Instruments Model 2000 X–Y recorder. For scan rates faster than 0.3 V/s a Tektronix Model 5511 oscilloscope coupled with a Tektronix C5-A camera was used. A laboratory built Pt rotating disk electrode was coupled with an IBM Instrumental Model EC 1219 rotating disk electrode controller. A three-electrode system was used. This consisted of a Pt button working electrode, a Pt wire counterelectrode, and a saturated calomel electrode (SCE) as reference. To minimize aqueous contamination of the nonaqueous solution, the reference electrode was separated from the bulk solution by a fritted glass bridge filled with the solvent and supporting electrolyte. The compounds were sensitive to both oxygen and light and therefore all electrochemical measurements other than spectroelectrochemistry were carried out in darkness, either in a dry box (Model 43-2 coupled with Dri-Train Model HE-493) or on a vacuum line. The spectroelectrochemical measurements were carried out outside the drybox and in darkness. In these cases, the blank solution was deaerated with nitrogen for at least 10 min before introduction of the compound and a nitrogen blanket was maintained over the solution during the experiment in order to minimize the decomposition of the compound under study.

A laboratory built platinum thin-layer electrode[21] was used to perform spectroelectrochemical measurements. The potential was controlled by an IBM Instruments Model EC 225 voltammetric analyzer with use of a typical scan rate of 0.003 V/s. For these measurements, the concentration of supporting electrolyte was 0.3 M. A Tracor Northern Model 1710 holographic optical spectrometer multichannel analyzer was used for measuring the electronic absorption spectra. Spectra were recorded from 290 to 920 nm and resulted from the signal averaging of 100 sequential spectral acquisitions.

Chemicals. The synthesis of each σ-bonded Ge(IV) complex was carried out under an argon atmosphere with use of Schlenk techniques. Benzene and toluene were thoroughly dried and distilled from sodium–benzophenone under argon prior to use. The starting material was (P)GeCl_2, which was synthesized according to literature procedures.[9,10] Benzonitrile (PhCN) was used as a solvent for the photochemical, spectroelectrochemical, and electrochemical measurements. This solvent was obtained from Aldrich and was distilled from P_2O_5 under an inert atmosphere and under vacuum to prevent polymerization. Methylene chloride (CH_2Cl_2) was distilled from calcium hydride under nitrogen. Tetrahydrofuran (THF) (Aldrich) was distilled from CaH_2 and then from a mixture of benzophenone and sodium under nitrogen. The supporting electrolyte, tetra-*n*-butylammonium perchlorate (TBAP), was purchased from Aldrich Co. and twice recrystallized from ethanol, dried,

(7) Kanisawa, M.; Schroeder, H. A. *Cancer Res.* **1967**, *27*, 1192.
(8) Miyamoto, T. K.; Sugita, N.; Matsumoto, Y.; Sasaki, Y.; Konno, M. *Chem. Lett.* **1983**, 1695.
(9) Maskasky, J. E.; Kenney, M. E. *J. Am. Chem. Soc.* **1971**, *93*, 2060.
(10) Maskasky, J. E.; Kenney, M. E. *J. Am. Chem. Soc.* **1973**, *95*, 1443.
(11) Cloutour, C.; Lafargue, D.; Richards, J. A.; Pommier, J. C. *J. Organomet. Chem.* **1977**, *137*, 157.
(12) Cloutour, C.; Debaig-Valade, C.; Pommier, J. C.; Dabosi, G.; Martineau, M. *J. Organomet. Chem.* **1981**, *220*, 21.
(13) Cloutour, C.; Lafargue, D.; Pommier, J. C. *J. Organomet. Chem.* **1983**, *190*, 35.
(14) Cloutour, C.; Debaig-Valade, C.; Gacherieu, C.; Pommier, J. C. *J. Organomet. Chem.* **1984**, *269*, 239.
(15) Cloutour, C.; Lafargue, D.; Pommier, J. C. *J. Organomet. Chem.* **1978**, *161*, 327.
(16) Lançon, D.; Cocolios, P.; Guilard, R.; Kadish, K. M. *J. Am. Chem. Soc.* **1984**, *106*, 4472.
(17) Perree-Fauvet, M.; Gaudemer, A.; Boucly, P.; Devynck, J. *J. Organomet. Chem.* **1976**, *120*, 439.
(18) Dolphin, D.; Halko, D. J.; Johnson, E. *Inorg. Chem.* **1981**, *20*, 4348.
(19) Kadish, K. M.; Boisselier-Cocolios, B.; Cocolios, P.; Guilard, R. *Inorg. Chem.* **1985**, *24*, 2139.
(20) Kadish, K. M.; Boisselier-Cocolios, B.; Coutsolelos, A.; Mitaine, P.; Guilard, R. *Inorg. Chem.* **1985**, *24*, 4521.
(21) Lin, X. Q.; Kadish, K. M. *Anal. Chem.* **1985**, *57*, 1498.

Table II. IR and UV–Visible Data of (P)Ge(R)$_2$ and (P)GeCl$_2$

por-phyrin	axial ligand	IR data[a] (cm^{-1}) C–H				M–C	UV–visible data[b] λ (nm (ε × 10^{-4}))[c] N(0,0)	B(1,0)	B(0,0)	Q(2,0)	Q(1,0)	Q(0,0)
OEP	CH_3	2900				605	350 (5.5)	430 (10.7)	441 (34.6)	528 (0.4)	568 (1.7)	602 (0.2)
	C_6H_5	3040	3060	3080		365	354 (4.5)	430 (7.2)	442 (35.1)	525 (0.3)	565 (1.7)	600 (0.2)
	$CH_2C_6H_5$	2910	3020	3060	3080	355	362 (4.4)	424 (3.9)	448 (10.7)	537 (0.3)	574 (1.3)	605 (0.1)
	Cl^-							391 (2.4)	413 (32.6)	500 (0.4)	541 (1.4)	575 (1.4)
TPP	C_6H_5					340		428 (5.1)	451 (43.3)	559 (0.3)	596 (1.2)	641 (2.8)
	$CH_2C_6H_5$	3075	3110	3127		312		430 (3.7)	455 (22.2)	562 (0.3)	607 (0.6)	655 (1.5)
	Cl^-							408 (4.9)	429 (31.3)	520 (0.4)	559 (1.3)	599 (1.0)

[a] CsI pellets. [b] Solvent: benzonitrile. [c] ε in M^{-1} cm^{-1}.

Table III. ^1H NMR Data of (P)Ge(R)$_2$ (400 MHz)

por-phyrin[a]	axial ligand	R_1	R_2	protons of R_1 m/i[b]	protons of R_1 δ (ppm)	protons of R_2 m/i[b]	protons of R_2 δ (ppm)	protons of axial ligand m/i[b]	protons of axial ligand δ (ppm)
OEP	CH_3	H	C_2H_5	s/4	10.15	t/24	1.99	s/6	−7.76
						q/16	4.16		
	C_6H_5	H	C_2H_5	s/4	10.12	t/24	1.92	d/4 (*o*-H)	−0.12
						q/16	4.09	t/4 (*m*-H)	4.59
								t/2 (*p*-H)	5.14
	$CH_2C_6H_5$	H	C_2H_5	s/4	9.97	t/24	1.95	s/4 ($-CH_2-$)	−6.16
						q/16	4.10	d/4 (*o*-H)	1.89
								t/4 (*m*-H)	5.56
								t/2 (*p*-H)	5.96
TPP	C_6H_5	C_6H_5	H	m/12	7.70	s/8	8.92	d/4 (*o*-H)	0.42
				d/8	8.13			t/4 (*m*-H)	4.85
								t/2 (*p*-H)	5.34
	$CH_2C_6H_5$	C_6H_5	H	m/12	7.51	s/8	8.83	s/4 ($-CH_2-$)	−5.55
				d/8	8.16			t/4 (*o*-H)	2.33
								t/4 (*m*-H)	5.79
								t/2 (*p*-H)	6.10

[a] Solvent: $CDCl_3$, reference TMS. [b] Key: *m* = number of lines, *i* = number of protons, s = singlet, d = doublet, t = triplet, q = quartet, m = multiplet.

and stored in vacuo at 40 °C. Tetra-*n*-butylammonium hydroxide (TBA(OH)), which was 1.0 M in methanol, was purchased from Aldrich Co. and used directly.

Preparation of (P)Ge(R)$_2$, Where R = CH_3, C_6H_5, or $CH_2C_6H_5$. (P)Ge(R)$_2$ was prepared according to classical methods.[9,10] RMgBr (2 mmol) in ether was added dropwise to (P)GeCl$_2$ (0.74 mmol) in 200 mL of benzene or toluene. Stirring was maintained for 30 min and the solution was hydrolyzed with water. The organic layer was dried over $MgSO_4$ and evaporated to dryness under vacuum. The resulting solid was then recrystallized. Yields, recrystallization solvents, and elemental analysis appear in Table I.

Preparation of (OEP)Ge(C_6H_5)X, Where X = Cl^-, OH^-, or ClO_4^-. A solution of (OEP)Ge(C_6H_5)$_2$ in $CHCl_3$ in the absence of O_2 was submitted to radiation from a visible source and the reaction monitored for 4 h by UV–visible spectroscopy. After evaporation of the solvent (OEP)Ge(C_6H_5)Cl was formed and was used without recrystallization. The yield was ≃90%.

(OEP)Ge(C_6H_5)OH or (OEP)Ge(C_6H_5)ClO_4 was obtained from the reaction of (OEP)Ge(C_6H_5)Cl in benzene and an aqueous solution of KOH (10%) or $HClO_4$ (50%). After drying over Na_2SO_4 and evaporation to dryness, the resulting solid was used without recrystallization. The yield was close to 80%.

Results and Discussion

Spectroscopic Properties of Neutral (P)Ge(R)$_2$. Figure 1 shows the electronic absorption spectra of (OEP)Ge(C_6H_5)$_2$ and (OEP)GeCl$_2$ in PhCN and electronic absorption data of each (P)Ge(R)$_2$ complex are given in Table II. In contrast to σ-bonded gallium[22] and indium[23,24] porphyrins, the electronic absorption spectra of (P)Ge(R)$_2$ belong to the "normal" class. Comparison of the (OEP)Ge(R)$_2$ spectra with (OEP)GeCl$_2$ indicates a 30–40 nm red shift of the Soret band and new morphology of the Q-bands for the σ-bonded species. The same difference in spectra is noted between chloro and the σ-bonded Ge(IV) derivatives in the tetraphenylporphyrin series. In this case, there is about a 20 nm red shift for the Soret band of (TPP)Ge(R)$_2$ and a 30–40 nm shift for the Q-bands. Similar shifts of wavelength maxima have already been reported for gallium[22] and indium[23,24] chloro and σ-bonded porphyrins.

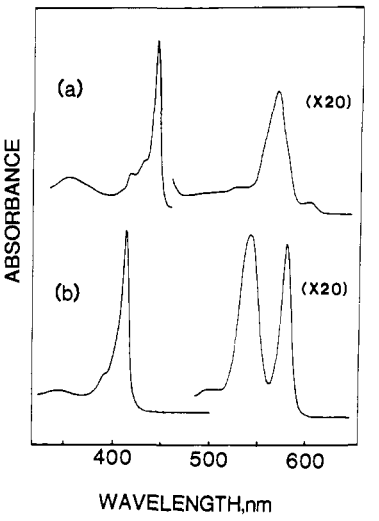

Figure 1. Electronic absorption spectra of (a) (OEP)Ge(C_6H_5)$_2$ and (b) (OEP)GeCl$_2$ in PhCN.

Characteristic IR vibrations can easily be assigned and IR data of these complexes are listed in Table II. Vibrational frequencies of the germanium–methyl and the germanium–aryl groups appear in the range of 312 to 605 cm^{-1}. Higher frequencies are also seen for the C–H stretching mode. These are between 2900 and 3000 cm^{-1} for the aliphatic C–H stretch and above 3000 cm^{-1} for the aromatic C–H stretch.

^1H NMR data of (P)Ge(R)$_2$ are summarized in Table III. The spectra show an upfield shift of the proton resonances of the alkyl or aryl ligands bonded to the metal. The methyl proton resonance signal of (OEP)Ge(CH_3)$_2$ appears at −7.76 ppm. A similar

(22) Coutsolelos, A.; Guilard, R. *J. Organomet. Chem.* **1983**, *253*, 273.
(23) Cocolios, P.; Guilard, R.; Fournari, P. *J. Organomet. Chem.* **1979**, *179*, 311.
(24) Tabard, A.; Guilard, R.; Kadish, K. M. *Inorg. Chem.* **1986**, *25*, 4277.

Table IV. ^{1}H NMR Data of (OEP)Ge(C_6H_5)X in $CDCl_3$ (300 MHz)

anionic ligand, X^-	meso H		methylenic H		methylic H		phenylic H	
	m/i^a	δ (ppm)	m/i^a	δ (ppm)	m/i^a	δ (ppm)	m/i^a	δ (ppm)
ClO_4^-	s/4	10.41	m/16	4.22	t/24	1.95	d/2	1.22
							t/2	5.31
							t/1	5.84
OH^{-b}	s/4	10.23	m/16	4.14	t/24	1.96	d/2	0.08
							t/2	4.70
							t/1	5.23
Cl^-	s/4	10.30	q/16	4.13	t/24	1.95	d/2	0.43
							t/2	4.86
							t/1	5.39

[a] Key: m = number of lines, i = number of protons, s = singlet, d = doublet, t = triplet, q = quartet, m = multiplet. [b] No signal observed for OH proton in $CDCl_3$, but in pyridine-d_5 $\delta_{H(hydroxyl\ group)} = -5.82$ ppm.

Table V. UV-Visible and IR Data of (OEP)Ge(C_6H_5)$_2$, (OEP)GeX_2, and (OEP)Ge(C_6H_5)X (where X = Cl^-, OH^-, or ClO_4^-)

axial ligand	axial ligand	IR data (cm^{-1})[a]		UV-visible data[d] λ (nm ($\epsilon \times 10^{-4}$))[e]					
		ν_{Ge-C}	ν_{Ge-X}	N(0,0)	B(1,0)	B(0,0)	Q(2,0)	Q(1,0)	Q(0,0)
C_6H_5	C_6H_5	365		354 (4.5)	430 (7.2)	442 (35.1)	525 (0.3)	565 (1.7)	600 (0.2)
C_6H_5	Cl^-	355	305	354 (4.2)	413 (4.7)	429 (21.9)	511 (0.2)	552 (1.6)	586 (0.7)
C_6H_5	OH^{-b}	350	580	353 (5.2)	405 (6.1)	426 (25.5)	511 (0.3)	550 (2.1)	584 (0.8)
C_6H_5	ClO_4^{-c}	355		357 (4.2)	390 (4.9)	411 (25.2)	506 (0.2)	541 (1.2)	578 (1.0)
Cl^-	Cl^-		314		391 (2.4)	413 (32.6)	500 (0.4)	541 (1.4)	575 (1.4)
OH^-	OH^-		634		387 (4.8)	407 (32.0)	496 (0.2)	534 (1.4)	570 (1.4)
ClO_4^-	ClO_4^-		315		384 (4.7)	404 (37.0)	500 (0.2)	534 (1.4)	571 (1.5)

[a] CsI pellets. [b] ν_{O-H}: 3260 cm^{-1}. [c] ν_{Cl-O}: 1080–1100 cm^{-1}. [d] Solvent: benzonitrile. [e] ϵ in M^{-1} cm^{-1}.

shielding has been reported for gallium and indium σ-bonded porphyrins.[22-24]

Chemical shifts of the aryl protons increase with the metal-proton length and the ortho protons of (OEP)Ge(C_6H_5)$_2$ appear at −0.12 ppm. The para-H resonance signal of the same complex occurs at 5.14 ppm. In contrast with the indium series, chemical shifts of the methinic or pyrrolic protons do not depend on the electron-withdrawing effect of axial ligand. The morphology of the ethylic proton signals of octaethylporphyrin derivatives is an A_2X_3 multiplet and it can be deduced that the metal is located in the mean plane of the four porphyrin nitrogens.[25]

Spectroscopic Study of (OEP)Ge(C_6H_5)X, Where X = Cl^-, OH^-, or ClO_4^-. Exposure of (OEP)Ge(C_6H_5)$_2$ in $CHCl_3$ to UV-visible radiation under argon leads to the spectral changes shown in Figure 2. The Soret band at 442 nm decreases while a new band is formed at 424 nm. At the same time the band at 565 nm decreases and is replaced by bands at 547 and 581 nm. The photochemical reaction was monitored by ^{1}H NMR in $CDCl_3$ and gave the spectra shown in Figure 3. In the absence of light, the phenyl protons of (OEP)Ge(C_6H_5)$_2$ are characterized by a doublet at −0.12 ppm, and two triplets at 4.59 and 5.14 ppm (Figure 3a). In the presence of light the signals for these resonances decrease and shift downfield to 0.43, 4.86, and 5.39 ppm. This is shown in Figure 3b. Integration of the phenyl signals shows a 50% decrease in intensity upon exposure to light and is consistent with the loss of one σ-bonded phenyl group on (OEP)Ge(C_6H_5)$_2$. A loss of one phenyl group is also indicated by the appearance of a new resonance at 7.36 ppm. This resonance can be accounted for by free benzene in solution.

Elemental analyses of the photochemically generated compound in $CHCl_3$ are consistent with the formula (OEP)Ge(C_6H_5)Cl ($C_{42}H_{49}N_4GeCl$, Found (calcd): C, 70.1 (70.27); H, 6.9 (6.88); Cl, 4.9 (4.91)), and this was confirmed by infrared spectroscopy before and after photolysis. The bisphenyl germanium(IV) complex has a germanium–carbon stretch at 365 cm^{-1}. The relative intensities of the peaks for Ge–C_6H_5 and Ge–Cl (see Figure 4a,b) give further evidence that (OEP)Ge(C_6H_5)Cl is the final product in the photolysis of (OEP)Ge(C_6H_5)$_2$.

Porphyrin analogues of (OEP)Ge(C_6H_5)X have been described in the literature. These are (TPP)Mo(C_6H_5)Cl[26] and (TPP)-

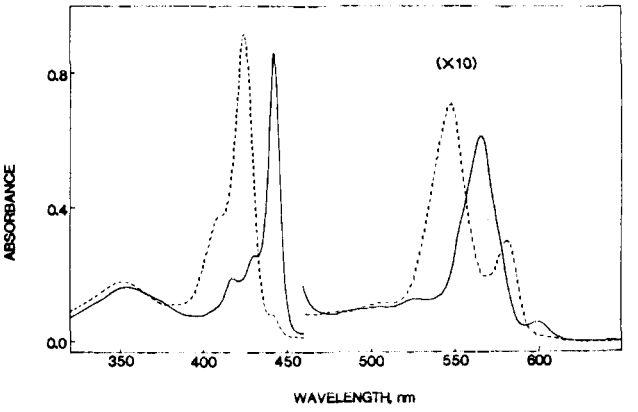

Figure 2. Electronic absorption spectra of (OEP)Ge(C_6H_5)$_2$ before (—) and after (---) photolysis in $CHCl_3$.

Rh(C_6H_5)Cl[27] which were identified on the basis of an X-ray structural analysis and (TPP)Sn(R)OH[14] (where R = ethyl, propyl, isopropyl, or isobutyl) which were characterized by ^{1}H NMR spectroscopy. These latter Sn compounds were formed during alkylation of (TPP)$SnCl_2$.

The molybdenum atom of (TPP)Mo(C_6H_5)Cl lies 0.089 Å out of the plane of the four nitrogens toward the chloride ligand[26] while the rhodium atom of (TPP)Rh(C_6H_5)Cl remains in the mean porphyrin plane.[27] On the basis of these results, it can be suggested that the germanium atom of (OEP)Ge(C_6H_5)Cl probably lies in the macrocyclic plane. In ^{1}H NMR, a quartet is observed for the methylenic protons of (OEP)Ge(C_6H_5)Cl as well in $CDCl_3$ and in pyridine-d_5. However, the methylenic protons of (OEP)Ge(C_6H_5)OH and (OEP)Ge(C_6H_5)ClO_4 are anisochronous. This could be explained by the greater anisotropy of the two axial ligands compared to those of (OEP)Ge(C_6H_5)Cl. Such results were already observed by Busby and Dolphin.[25]

Other (OEP)Ge(C_6H_5)X complexes were synthesized from (OEP)Ge(C_6H_5)Cl, and the presence of one phenyl group σ-bonded to Ge(IV) is also easily deduced from the ^{1}H NMR data. Resonances of the phenyl protons appear downfield in relation to resonances of the starting (OEP)Ge(C_6H_5)$_2$ complex. In addition, the chemical shifts of these protons vary with the elec-

(25) Busby, C. A.; Dolphin, D. *J. Magn. Reson.* **1976**, *23*, 211.
(26) Colin, J.; Chevrier, B. *Organometallics* **1985**, *4*, 1090.
(27) Fleischer, E. B.; Lavallee, D. *J. Am. Chem. Soc.* **1967**, *89*, 7132.

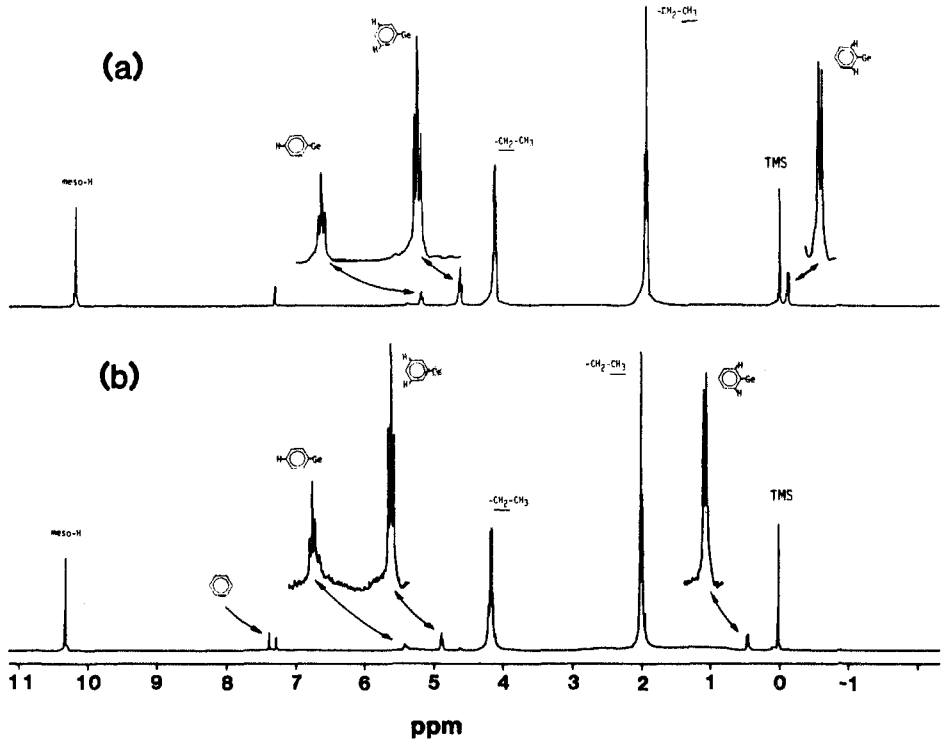

Figure 3. 400-MHz ^{1}H NMR spectra of (OEP)Ge(C_6H_5)$_2$ in $CDCl_3$ (a) in the dark and (b) after exposure to UV–visible radiation for 6 h.

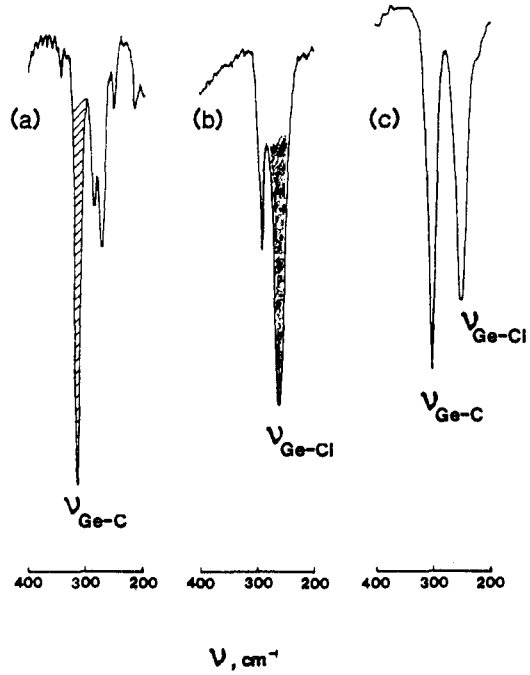

Figure 4. Infrared spectra (CsI pellets) of (a) (OEP)Ge(C_6H_5)$_2$, (b) (OEP)$GeCl_2$ and (c) (OEP)Ge(C_6H_5)Cl. Only the Ge–carbon and Ge–Cl regions are indicated.

tron-withdrawing nature of the anionic ligand bonded to the metal, i.e., the more basic the axial ligand, X^-, the higher the field. This results in the following sequence of phenylic proton resonances

(OEP)Ge(C_6H_5)OH < (OEP)Ge(C_6H_5)Cl < (OEP)Ge(C_6H_5)ClO_4

The same order is observed for the methinic proton resonance signals that occur at 10.23 ppm ($X = OH^-$), 10.30 ppm ($X = Cl^-$), and 10.41 ppm ($X = ClO_4^-$). These ^{1}H NMR data are summarized in Table IV.

The electronic absorption spectral data for seven different Ge(IV) complexes are summarized in Table V while Figure 5

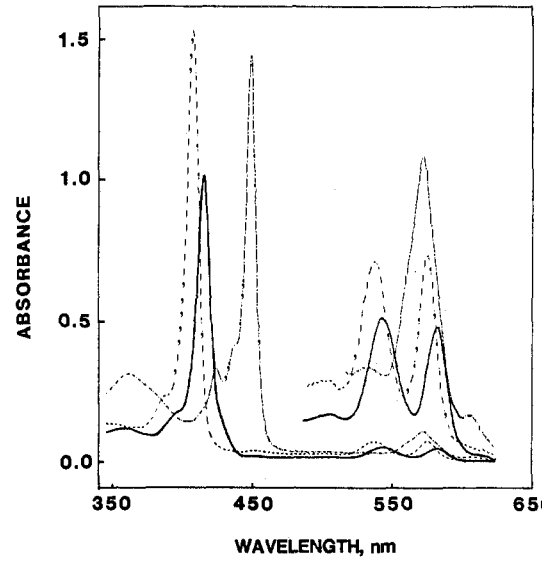

Figure 5. Electronic absorption spectra of (OEP)Ge(C_6H_5)ClO_4 (—), (OEP)Ge(ClO_4)$_2$ (- - -), and (OEP)Ge(C_6H_5)$_2$ (–·–) in PhCN.

shows the UV–visible spectra of (OEP)Ge(ClO_4)$_2$, (OEP)Ge(C_6H_5)ClO_4, and (OEP)Ge(C_6H_5)$_2$ in PhCN. The Soret band maximum is at 442 nm for (OEP)Ge(C_6H_5)$_2$, 411 nm for (OEP)Ge(C_6H_5)ClO_4, and 404 nm for (OEP)Ge(ClO_4)$_2$. The Soret (B(0,0)) bands of (OEP)Ge(C_6H_5)X range from 429 nm ($X = Cl^-$) to 411 nm ($X = ClO_4^-$) and follow the order $Cl^- > OH^- > ClO_4^-$. These Soret band maxima are between that of (OEP)Ge(C_6H_5)$_2$ (442 nm) and of (OEP)GeX_2, the latter of which also shift in the order $Cl^- > OH^- > ClO_4^-$ and varies between 413 and 404 nm.

IR spectral data of the (OEP)Ge(C_6H_5)X complexes are given in Table V. Assignments of the characteristic stretching modes are straightforward. The position of the germanium anionic ligand vibration can be unambiguously given for (OEP)Ge(C_6H_5)OH (ν_{Ge-OH} = 580 cm^{-1}) and (OEP)Ge(C_6H_5)Cl (ν_{Ge-Cl} = 305 cm^{-1}). On the other hand, a ν_{Ge-ClO_4} stretch could not be assigned for (OEP)Ge(C_6H_5)ClO_4. Nevertheless, the presence of a ClO_4^- group complexed to Ge(IV) is certain. Vibrational stretching

Table VI. Chemical Shifts of R Protons for (P)Ge(R)$_2$ in $CDCl_3$ before and after Exposure to Visible Light (300 MHz)

por-phyrins	ligand	ligand	conditions	δ (-CH_2-)	δ (-CH_3)	δ (*o*-H)	δ (*m*-H)	δ (*p*-H)	δ (meso H or pyrr H)
OEP	CH_3	CH_3	dark		-7.76				10.15
	CH_3	Cl^-	light[a]		-6.87				10.32
	C_6H_5	C_6H_5	dark			-0.12	4.59	5.14	10.12
	C_6H_5	Cl^-	light[a]			0.43	4.86	5.39	10.30
	$CH_2C_6H_5$	$CH_2C_6H_5$	dark	-6.16		1.89	5.56	5.96	9.97
	$CH_2C_6H_5$	Cl^-	light[a]	-5.37		overlapped	5.77	6.11	10.25
TPP	CH_2CH_3	CH_2CH_3	dark[b]	-6.66	-4.28				
	CH_2CH_3	$O_2CH_2CH_3$	light + O_2[b]	-6.75, -0.48	-3.95, -0.81				
	$O_2CH_2CH_3$	$O_2CH_2CH_3$	light + O_2[b]	-0.48	-0.81				
	C_6H_5	C_6H_5	dark			0.42	4.85	5.34	8.92
	C_6H_5	Cl^-	light[a]			0.49	5.07	5.54	9.06
	$CH_2C_6H_5$	$CH_2C_6H_5$	dark	-5.55		2.33	5.79	6.10	8.83
	$CH_2C_6H_5$	Cl^-	light[a]	-4.37		2.63	5.96	6.32	9.00

[a] Compound generated by exposure of (P)Ge(R)$_2$ to light in the absence of O_2. [b] From ref 15.

modes of the ClO_4^- group appear in the range of 1080–1100 cm^{-1} and agree with data in the literature.[28]

Table VI lists ^1H NMR chemical shifts of (P)Ge(R)$_2$ before and after irradiation. As seen in this table there is a dramatic downfield shift of the alkyl protons of (TPP)Ge(CH_2CH_3)$_2$[15] upon going to the oxygen insertion products (TPP)Ge(CH_2CH_3)(OO-CH_2CH_3) and (TPP)Ge($OOCH_2CH_3$)$_2$ (from -6.66 to -0.48 ppm for $-CH_2-[\alpha]$ and from -4.28 to -0.81 ppm for $-CH_3[\beta]$). However, the alkyl protons bonded to the metal are shifted downfield only slightly upon going from the σ-dialkyl(aryl) to the σ-monoalkyl(aryl) complex, i.e., from -6.66 to -6.15 ppm for $-CH_2-[\alpha]$ and from -4.28 to -3.95 ppm for $-CH_3[\beta]$. The same trend is observed in the present series of compounds. For example, the methyl protons of (OEP)Ge(CH_3)$_2$ shift from -7.76 to -6.87 ppm upon cleavage of one σ-bonded CH_3 group. The data in Table VI also show that no peroxide is formed under our experimental conditions.

Additional evidence for homolytic cleavage of a germanium–carbon bond in (P)Ge(R)$_2$ upon irradiation is given by gas chromatographic analysis of the products. Photolysis of (OEP)Ge(CH_3)$_2$ in both THF or CH_2Cl_2 indicates production of methane gas, but no ethane is detected. Also, benzene is detected by GC and ^1H NMR spectroscopy after irradiation of (P)Ge(C_6H_5)$_2$. Benzene is also detected after irradiation of (P)Ge($CH_2C_6H_5$)$_2$ in CH_2Cl_2 and toluene is only observed in very small quantities. This is not surprising if one considers the relative stability of phenyl and benzyl radicals.

Electrode Reactions of (OEP)Ge(C_6H_5)X, Where X = ClO_4^-, OH^-, and Cl^-. Cyclic voltammograms of (OEP)Ge(C_6H_5)ClO_4, (OEP)Ge(C_6H_5)OH, and (OEP)Ge(C_6H_5)Cl in PhCN, 0.1 M TBAP, are shown in Figure 6. The voltammogram of (OEP)-Ge(C_6H_5)ClO_4 is shown in Figure 6a. Two reversible one-electron reductions (processes 2 and 3) occur at $E_{1/2}$ = -0.82 V and $E_{1/2}$ = -1.30 V. Both processes 2 and 3 are characterized by $|E_{pa} - E_{pc}|$ = 60 mV. The ratio of $i_p/v^{1/2}$ is constant for both waves, indicating diffusion-controlled processes. Figure 6a also shows the presence of one oxidation (process 1). This reversible, diffusion-controlled oxidation occurs at $E_{1/2}$ = +1.40 V.

(OEP)Ge(C_6H_5)Cl has two reduction waves at $E_{1/2}$ = -0.89 and -1.30 V (Figure 6b). In addition, there are oxidation waves at E_p = +1.10 V and $E_{1/2}$ = +1.40 V. The irreversible oxidation at 1.10 V involves oxidation of chloride ion bound to (OEP)Ge-(C_6H_5)Cl.[29] The second oxidation of (OEP)Ge(C_6H_5)Cl is at an identical potential as for oxidation of (OEP)Ge(C_6H_5)ClO_4 in PhCN thus providing further evidence for oxidation of Cl^- on (OEP)Ge(C_6H_5)Cl and formation of (OEP)Ge(C_6H_5)ClO_4 after the abstraction of one electron. UV–visible spectra of (OEP)-Ge(C_6H_5)Cl were taken in PhCN and in PhCN containing between 0.01 and 1.50 M TBAP and suggest that Cl^- replacement

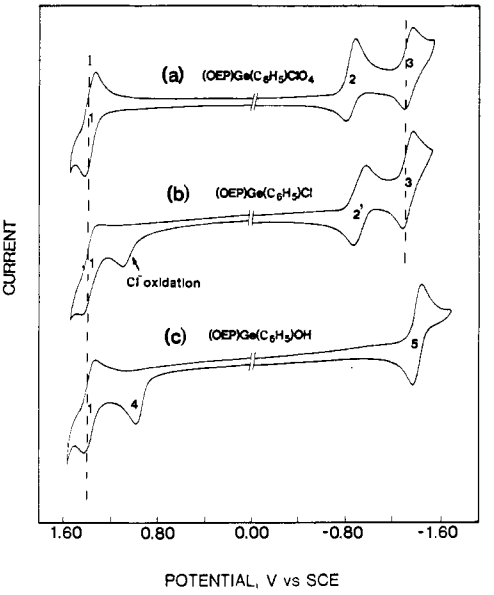

Figure 6. Cyclic voltammograms of (a) 10^{-3} M (OEP)Ge(C_6H_5)ClO_4, (b) 10^{-3} M (OEP)Ge(C_6H_5)Cl, and (c) 10^{-3} M (OEP)Ge(C_6H_5)OH in PhCN (0.1 M TBAP) at 0.1 V/s.

only occurs at supporting electrolyte concentrations approaching 1.0 M. This ligand exchange under these conditions is given by the following reaction.

$$(OEP)Ge(C_6H_5)Cl + ClO_4^- \rightleftarrows (OEP)Ge(C_6H_5)ClO_4 + Cl^- \quad (1)$$

The chloride anion is still associated to $[(OEP)Ge(C_6H_5)]^+$ in PhCN containing 0.1 M TBAP and the first reduction potential is shifted from -0.82 V for X = ClO_4^- to -0.89 V for X = Cl^-. (OEP)Ge(C_6H_5)OH differs from (OEP)Ge(C_6H_5)ClO_4 and (OEP)Ge(C_6H_5)Cl in that the OH^- ligand is completely associated at all concentrations of TBAP. (OEP)Ge(C_6H_5)OH is reversibly reduced in PhCN, 0.1 M TBAP, at $E_{1/2}$ = -1.38 V. This is shown in Figure 6c where the reduction is labeled as process 5. Analysis of the current–voltage curves indicates that this reduction is a diffusion-controlled one-electron process. Two oxidations of (OEP)Ge(C_6H_5)OH are also observed in the potential range of PhCN. The first oxidation is not reversible and at a scan rate of 0.1 V/s occurs at E_p = +1.0 V. This oxidation is not coupled to a rereduction peak. The shape and height of the oxidation peak are indicative of a diffusion-controlled one-electron transfer. The peak shape is characterized by $|E_p - E_{p/2}|$ = 60 mV while $i_p/v^{1/2}$ is constant. All of these data are also consistent with an initial diffusion-controlled one-electron oxidation process that is followed by a rapid chemical reaction. As will be shown in the following sections, this irreversible reaction corresponds to the oxidation of bound OH^- ligand to generate the (OEP)Ge(C_6H_5)ClO_4 complex which is then further oxidized at +1.40 V. This process

(28) Nakamoto, K. *Infrared and Raman Spectra of Inorganic and Coordination Compounds*; Wiley: New York, 1978.

(29) Cl^- is irreversibly oxidized at E_{pa} = +1.10 V (SCE) in PhCN, 0.1 M TBAP at 0.1 V/s.

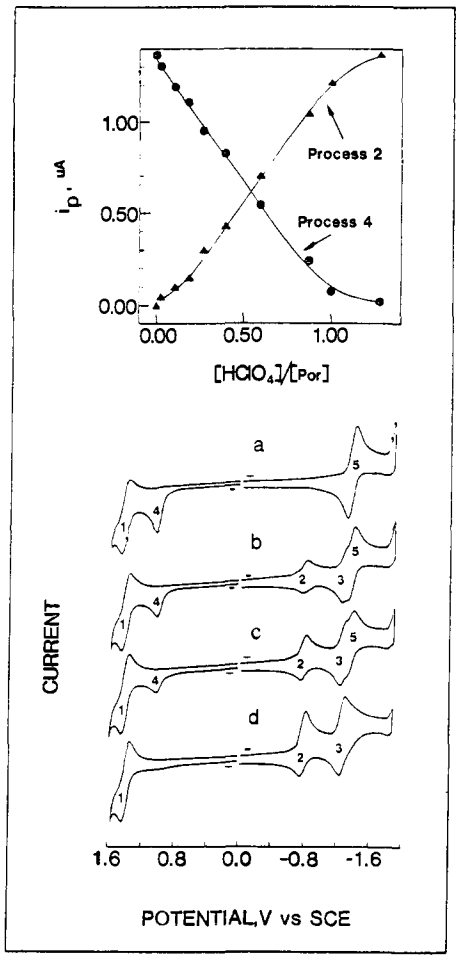

Figure 7. Cyclic voltammograms of 1.43×10^{-3} M (OEP)Ge(C_6H_5)OH in PhCN (0.1 M TBAP) containing various concentrations of $HClO_4$: (a) 0.0 M; (b) 5.85×10^{-4} M; (c) 1.25×10^{-3} M; and (d) 1.43×10^{-3} M. Insert shows the plot of peak current for reaction 4 (●) and reaction 2 (▲) as a function of [$HClO_4$].

is labeled as process 1 in Figure 6c. The oxidation of bound OH^- on (OEP)Ge(C_6H_5)OH is labeled as process 4 in Figure 6c and is represented by the following set of reactions.

$$(OEP)Ge(C_6H_5)OH \rightleftarrows [(OEP)Ge(C_6H_5)OH]^+ + e \quad (2a)$$

$$[(OEP)Ge(C_6H_5)OH]^+ \rightarrow [(OEP)Ge(C_6H_5)]^+ + {}^{\bullet}OH \quad (2b)$$

The formation of $[(OEP)Ge(C_6H_5)]^+$ or (OEP)Ge(C_6H_5)ClO_4 after the one-electron oxidation of (OEP)Ge(C_6H_5)OH was identified by both its electrochemistry as well as its characteristic UV–visible spectra. The generated ·OH radical was not characterized in solution but most likely reacted with the electrode to give PtO. Further evidence for the involvement of ·OH in the reaction was also given by monitoring cyclic voltammograms of (OEP)Ge(C_6H_5)OH as a function of increasing H^+ concentration in solution. This is discussed in the following section.

Electrochemically Monitored Titrations of (OEP)Ge(C_6H_5)OH with $HClO_4$. Figure 7 demonstrates changes that occur in the cyclic voltammogram of (OEP)Ge(C_6H_5)OH upon the addition of $HClO_4$. The cyclic voltammogram in the absence of $HClO_4$ is characterized by a reversible reduction wave at $E_{1/2} = -1.38$ V (process 5), an irreversible oxidation wave at $E_p = +1.0$ V (process 4), and a reversible oxidation wave at $E_{1/2} = +1.40$ V (process 1). Upon addition of $HClO_4$ to solutions containing (OEP)Ge(C_6H_5)OH, new reductions are observed at $E_{1/2} = -0.82$ (process 2) and −1.30 V (process 3). This is shown in Figure 7b. The currents for process 2 and process 3 increase as the concentration of $HClO_4$ is increased. There is also a simultaneous decrease in current for the reduction at $E_{1/2} = -1.38$ V (process 5) as well as for the oxidation peak at $E_p = +1.0$ V (process 4). At the same time, the second oxidation (process 1) at $E_{1/2} = +1.40$ V remains unchanged. This indicates the formation of (OEP)-Ge(C_6H_5)ClO_4 as shown by eq 3.

$$(OEP)Ge(C_6H_5)OH + HClO_4 \rightleftarrows (OEP)Ge(C_6H_5)ClO_4 + H_2O \quad (3)$$

The maximum peak currents for processes 2 and 4 are shown in Figure 7 as a function of the $HClO_4$/porphyrin ratio. As seen in Figure 7, the acid–base reaction shown in eq 3 is complete after 1 equiv of $HClO_4$ has been added, at which point the reactions at $E_p = +1.0$ V and $E_{1/2} = -1.38$ V have disappeared. The cyclic voltammogram is then characterized by two reversible reductions at −0.82 and −1.30 V and a single reversible oxidation at +1.40 V (see Figure 7d). The spectrum of the solution after addition of 1 equiv of $HClO_4$ indicates complete formation of (OEP)Ge-(C_6H_5)ClO_4. The resulting compound has a Soret band at 410 nm and two Q-bands at 539 and 578 nm. Thus the spectral and electrochemical data suggest the electrode and ligand addition reactions described in Scheme I. Moreover, it is also possible to convert (OEP)Ge(C_6H_5)ClO_4 to (OEP)Ge(C_6H_5)OH by controlled-potential electrolysis. The current for the reduction at −1.30 V decreases and a reduction wave at $E_{1/2} = -1.38$ V appears if the potential is held at −1.2 V for 15 min and scanned negatively. This suggests that an EC mechanism is involved, generating the starting compound, (OEP)Ge(C_6H_5)OH.

Electroreduction of (OEP)Ge(R)$_2$ and (TPP)Ge(R)$_2$. Similar reductive electrochemical behavior is observed for each of the investigated (P)Ge(R)$_2$ complexes in PhCN. Either one or two reversible single-electron additions occur without cleavage of the germanium–carbon bond on the cyclic voltammetric time scale. Potentials for these reductions are given in Table VIII.

Each of the (OEP)Ge(R)$_2$ complexes is reduced by one electron in the potential range of PhCN while each (TPP)Ge(R)$_2$ complex undergoes two reductions in the potential range of the solvent.

Table VII. Half-Wave and Peak Potentials for (OEP)Ge(C_6H_5)X in PhCN (0.1 M TBAP)

complex	oxidation		reduction	
(OEP)Ge(C_6H_5)ClO_4	+1.40		−0.82	−1.30
(OEP)Ge(C_6H_5)OH	+1.40	+1.00[a]		−1.38
(OEP)Ge(C_6H_5)Cl	+1.40	+1.10[a,b]	−0.89	−1.30

[a] E_{pa} measured at 0.1 V/s. [b] Corresponds to oxidation of bound Cl^- in solution.

Table VIII. Half-Wave and Peak Potentials (V versus SCE) of (P)Ge(R)$_2$ in PhCN (0.1 M TBAP)

		oxidation		reduction	
porphyrin	ligand	$E_{1/2}$	E_{pa}[a]	$E_{1/2}$	$E_{1/2}$
OEP	$CH_2C_6H_5$	1.34[a]	0.64	−1.54	
	CH_3	1.37	0.75	−1.48	
	C_6H_5	1.39	0.88	−1.40	
TPP	$CH_2C_6H_5$	1.34[a]	0.73	−1.17	−1.72
	C_6H_5	1.45	0.95	−1.10	−1.65

[a] E_{pa} measured at 0.10 V/s.

Scheme I

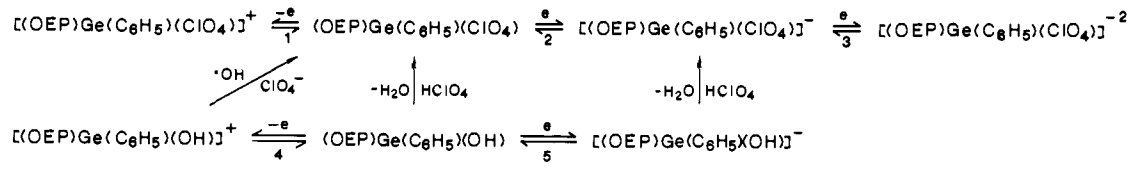

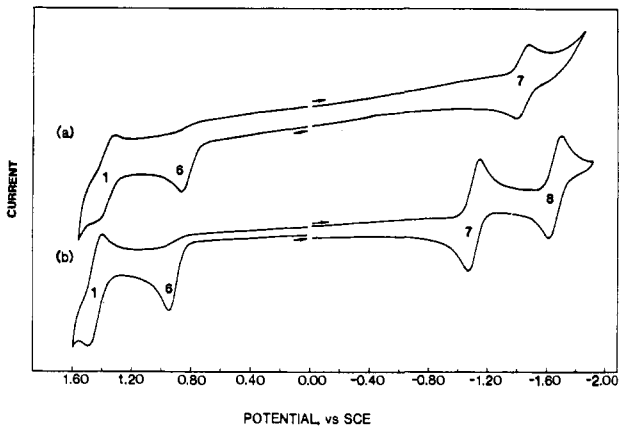

Figure 8. Cyclic voltammograms of (a) 10^{-3} M $(OEP)Ge(C_6H_5)_2$ and (b) 10^{-3} M $(TPP)Ge(C_6H_5)_2$ in PhCN (0.1 M TBAP) at 0.1 V/s.

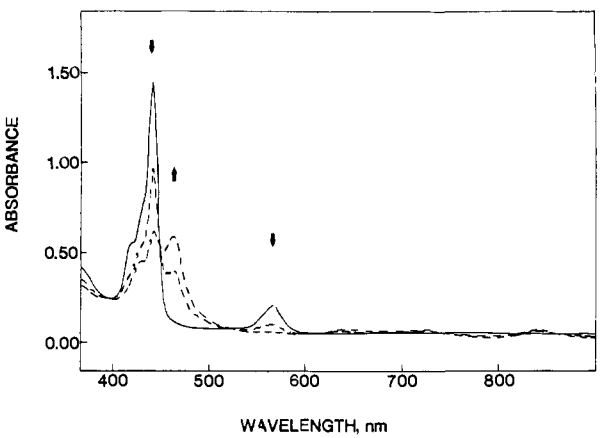

Figure 9. Electronic absorption spectra taken during the reduction of $(OEP)Ge(C_6H_5)_2$ in PhCN (0.3 M TBAP).

This is illustrated for $(TPP)Ge(C_6H_5)_2$ and $(OEP)Ge(C_6H_5)_2$ in Figure 8. The single reduction of $(OEP)Ge(C_6H_5)_2$ (process 7, Figure 8a) is characterized by a peak-to-peak potential separation $|E_{pa} - E_{pc}| = 60$ mV at 0.1 V/s and a peak current ratio $i_{pa}/i_{pc} = 1.0$. A plot of i_p against $v^{1/2}$ is linear. Bulk coulometry at −1.7 V gives 1.0 electron transferred in this process. Thus, all of the data suggest a diffusion-controlled reversible one-electron transfer.

Reversible one-electron reductions also occur for $(OEP)Ge(CH_3)_2$ and $(OEP)Ge(CH_2C_6H_5)_2$. The second reduction of $(OEP)Ge(R)_2$ is expected to occur at about −1.9 V versus SCE, but this potential is just at the cathodic limit of the solvent and a second reduction was not observed.

Diffusion-controlled reversible one-electron transfers are also observed for the $(TPP)Ge(R)_2$ complexes. The first reduction of $(TPP)Ge(C_6H_5)_2$ (process 7, Figure 8b) occurs at an $E_{1/2}$ value which is 380 mV more positive than that for reduction of $(OEP)Ge(C_6H_5)_2$. This is due to the decreased basicity of the TPP ring with respect to OEP. A second reduction of $(TPP)Ge(C_6H_5)_2$ (process 8) occurs at −1.65 V while $(TPP)Ge(CH_2C_6H_5)_2$ has a second reduction at −1.72 V.

It is not surprising that the diaryl germanium complexes are more easily reduced than the dialkyl complexes if one considers how the substituent R affects the electron density on the porphyrin macrocycle of $(P)Ge(R)_2$. The Hammett substituent constant of CH_3 is 0.00 and that of C_6H_5 is 0.60. Differences in $E_{1/2}$ between the first reduction of $(P)In(CH_3)$ and $(P)In(C_6H_5)$[19] (where P = TPP or OEP) range from 20 to 30 mV. $(OEP)Ge(C_6H_5)_2$ is more easily reduced than $(OEP)Ge(CH_3)_2$ by 80 mV. The two alkyl or two aryl groups on $(P)Ge(R)_2$ thus triple the overall substituent effect observed for (P)In(R).

Thin-layer cyclic voltammograms of $(P)Ge(R)_2$ confirm that a cleavage of the germanium–carbon bond does not occur after the addition of one electron. Well-defined thin-layer cyclic voltammograms are obtained and the time-resolved electron-absorption spectra during the reduction of $(OEP)Ge(C_6H_5)_2$ are shown in Figure 9.

The electronic absorption spectrum of $(OEP)Ge(C_6H_5)_2$ shows small amounts of decomposition in solution. Upon reduction of the complex by one electron the Soret band of $(OEP)Ge(C_6H_5)_2$ moves from 444 to 466 nm. At the same time the Q-band at 568 nm disappears and two new peaks appear at 728 and 843 nm. Isobestic points are observed at 528 and 616 nm, indicating that two species, $(OEP)Ge(C_6H_5)_2$ and $[(OEP)Ge(C_6H_5)_2]^{+\cdot}$, are in equilibrium. The position and intensity of the new bands and the two absorption peaks at 728 and 843 nm suggest the formation of a porphyrin π-anion radical. The original spectrum of $(OEP)Ge(C_6H_5)_2$ could be obtained by re-oxidation, indicating that the reduction is not only electrochemically but also spectroelectrochemically reversible.

Spectral changes associated with reduction of $(TPP)Ge(C_6H_5)_2$ are similar to those observed after reduction of $(OEP)Ge(C_6H_5)_2$. This is shown in Table IX. After the addition of one electron, the Soret peak at 451 nm decreases in intensity and shifts to 484 nm. At the same time, the visible bands at 596 and 641 nm disappear and are replaced by two broad absorbances with maxima at 733 and 819 nm. Isobestic points are observed at 455, 579, and 688, indicating the lack of any detectable spectral intermediates during the electroreduction. The reduction of $(TPP)Ge(C_6H_5)_2$ is also spectrally reversible and the starting species could be regenerated by reversing the applied potential.

Table IX. Peak Maximum Wavelengths and Their Molar Absorptivities for $(OEP)Ge(C_6H_5)_2$ and $(TPP)Ge(C_6H_5)_2$ in PhCN (0.3 M TBAP)

		λ_{max}, nm ($\epsilon \times 10^{-4}$)		
			Q-band	
compd	reaction	Soret band		
$(OEP)Ge(C_6H_5)_2$	none	444 (23.6)	568 (2.0)	
	1st reduction	466 (9.0)	728 (0.7)	843 (0.4)
	1st oxidation	410 (27.7)	539 (2.0)	578 (2.0)
	re-reduction	426 (30.8)	550 (3.5)	584 (1.6)
$(TPP)Ge(C_6H_5)_2$	none	451 (40.8)	596 (1.3)	641 (2.8)
	1st reduction	484 (11.2)	733 (0.6)	819 (1.4)

Finally, further evidence of porphyrin π-anion radical formation in the first reduction of $(P)Ge(R)_2$ was obtained by ESR measurements. For example, bulk electrolysis of $(OEP)Ge(C_6H_5)_2$ at −1.7 V gave an ESR signal with a g value of 2.003 and ΔH_{pp} of 6.3 G.

Electrooxidation of $(OEP)Ge(R)_2$ and $(TPP)Ge(R)_2$. All five $(P)Ge(R)_2$ compounds undergo two oxidations, the first of which is irreversible. This is shown in Figure 8a for the case of $(OEP)Ge(C_6H_5)_2$. The first oxidation (process 6) occurs at $E_p = +0.88$ V. The value of $i_{pa}/v^{1/2}$ is constant and current integration at +1.15 V gives a value of 1.0 electron transferred. These data are consistent with an initial diffusion-controlled one-electron oxidation process that is followed by a rapid chemical reaction. The other four investigated complexes also undergo diffusion-controlled oxidations that are coupled with a rapid chemical reaction following electron abstraction. In all cases the second oxidation (process 1) is a reversible diffusion-controlled one-electron transfer.

When the positive potential scan is reversed at +1.2 V, two additional reductions are obtained. For the case of $(OEP)Ge(C_6H_5)_2$ these occur at $E_{1/2} = -0.82$ and −1.30 V (see Figure 10a). The peak potential separations, $|E_{pa} - E_{pc}|$, are equal to 60 mV at 0.1 V/s. The value of i_{pa}/i_{pc} is 1.0 at a scan rate of 0.1 V/s. This fact and the constant ratio of $i_p/v^{1/2}$ indicates that the reductions involve diffusion-controlled one-electron transfers. The $E_{1/2}$ values for the new reductions are the same as those of $(OEP)Ge(C_6H_5)ClO_4$ (see Table VII) and thus suggest that this species is generated after cleavage of one Ge–C bond on $(OEP)Ge(C_6H_5)_2$.

If 1 equiv of TBA(OH) is added to solutions of $(OEP)Ge(C_6H_5)_2$, the two additional reductions that occur after oxidation disappear. However, a new reversible reduction (process 5) is observed at $E_{1/2} = -1.38$ V. This is consistent with conversion

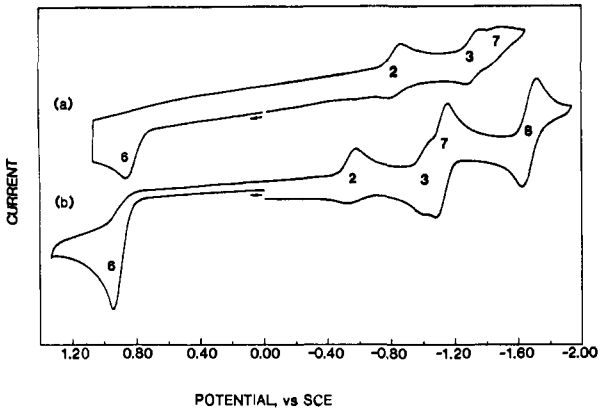

Figure 10. Cyclic voltammograms of (a) 10^{-3} M (OEP)Ge(C_6H_5)$_2$ and (b) 10^{-3} M (TPP)Ge(C_6H_5)$_2$ in PhCN (0.1 M TBAP) at 0.1 V/s.

Table X. Half-Wave Potentials (V versus SCE) for Reduction of Electrogenerated (P)Ge(R)ClO_4 in PhCN (0.1 M TBAP)

porphyrin	ligand	$E_{1/2}$	$E_{1/2}$
OEP	$CH_2C_6H_5$	−0.86	−1.36
	CH_3	−0.88	−1.29
	C_6H_5	−0.82	−1.30
TPP	$CH_2C_6H_5$	−0.57	−1.05
	C_6H_5	−0.55	−1.02

of electrochemically generated (OEP)Ge(C_6H_5)ClO_4 to (OEP)-Ge(C_6H_5)OH and suggests the following overall mechanism for the oxidation/reduction of (OEP)Ge(C_6H_5)$_2$ (Scheme II).

Figure 8b shows a typical cyclic voltammogram of (TPP)Ge-(C_6H_5)$_2$ and Figure 10b shows another example of the similar mechanism which occurs for (TPP)Ge(C_6H_5)$_2$. When the scan is reversed at +1.3 V, additional reductions are observed at $E_{1/2}$ = −0.57 V (process 2) and −1.14 V (process 3). The product after the first oxidation of (TPP)Ge(C_6H_5)$_2$ can be assigned as (TP-P)Ge(C_6H_5)ClO_4. All five investigated complexes exhibit similar behavior and differ only in the values of their half-wave and peak potentials. These potentials are summarized in Table X.

Spectroelectrochemistry of (OEP)Ge(C_6H_5)$_2$. The postulated sequence of reactions shown in Scheme II was confirmed by spectroelectrochemical measurements taken during (OEP)Ge-(C_6H_5)$_2$ oxidation/reduction. A typical thin-layer cyclic voltammogram is shown in Figure 11. The resulting reduction (process 2) at E_p = −0.80 V is irreversible after electrooxidation at a scan rate of 0.003 V/s. This is in contrast to that observed at 0.1 V/s (see Figure 10).

The initial one-electron oxidation product of (OEP)Ge(C_6H_5)$_2$ and the species to which it chemically converts before abstraction of a second electron at more positive potentials were also monitored by thin-layer spectroelectrochemistry. Voltage-resolved electronic absorption spectra of each complex were recorded in darkness and are shown in Figure 12a for the initial electrooxidation of (OEP)Ge(C_6H_5)$_2$ in PhCN. Upon the abstraction of one electron, the Soret band shifts from 444 to 410 nm and the Q-band split into two bands at 539 and 578 nm. This spectrum is characteristic of a Ge(IV) porphyrin.

Abstraction of one electron from the macrocycle of (OEP)-Ge(C_6H_5)$_2$ weakens the Ge–C_6H_5 bond which heterolytically

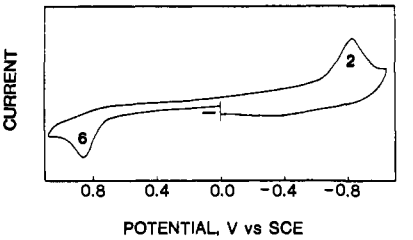

Figure 11. Thin-layer cyclic voltammogram of 10^{-3} M (OEP)Ge(C_6H_5)$_2$ in PhCN (0.3 M TBAP).

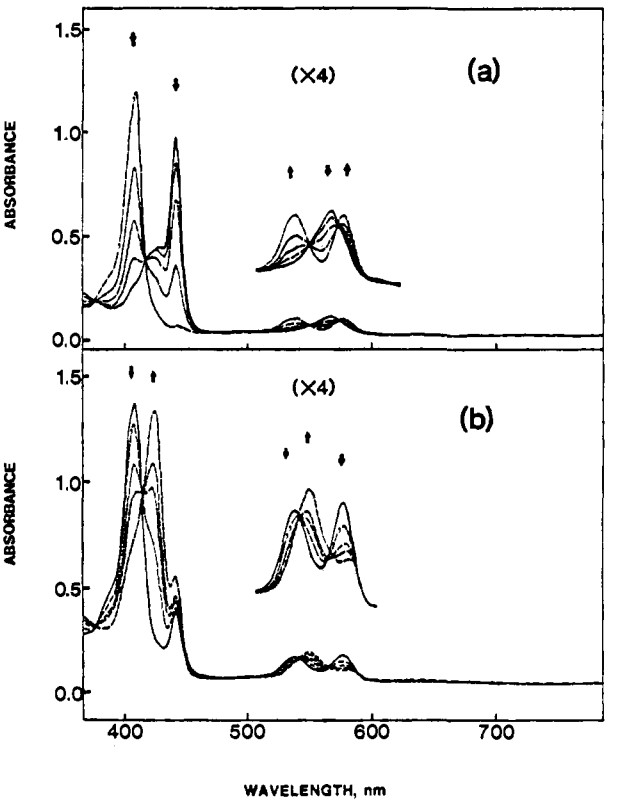

Figure 12. Voltage-resolved electronic absorption spectra of (OEP)Ge-(C_6H_5)$_2$ in PhCN (0.3 M TBAP): (a) for initial oxidation and (b) for reduction of the electrooxidized species.

cleaves thus generating a phenyl radical. The final spectrum presented in Figure 12a is identical with that of (OEP)Ge-(C_6H_5)ClO_4. This chemical reaction was so fast that two isobestic points are observed at 418 and 550 nm.

Upon reduction of the newly generated species at $E_{1/2}$ = −0.82 V, the Soret band peak moves back to 426 nm. The two bands in the visible region completely disappear and two new peaks appear at 550 and 584 nm. No isobestic points are obtained, suggesting that more than two species are present in solution (see Figure 12b). The identity of the final spectrum resembles (OEP)Ge(C_6H_5)OH and indicates that trace water in the solution is reduced by one electron to generate OH^- and H_2. A detailed mechanism of this reduction will be discussed elsewhere.[30] The

Scheme II

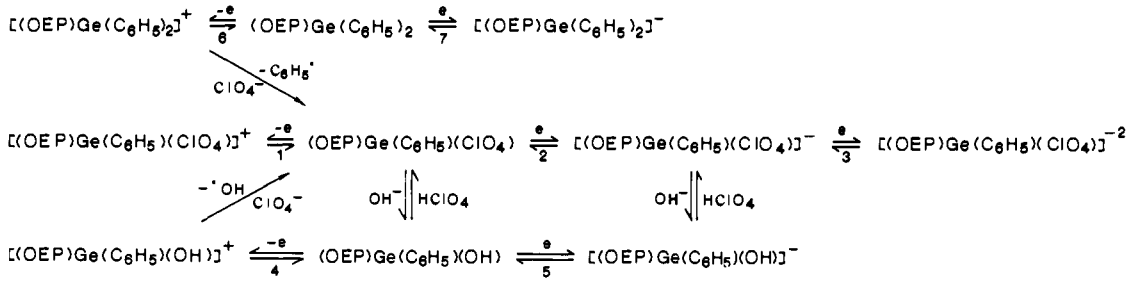

spectral data for $(OEP)Ge(C_6H_5)_2$ and its oxidation and reduction products are summarized in Table IX.

The second oxidation of $(OEP)Ge(C_6H_5)_2$ (process 1) occurs at the same half-wave potential as for oxidation of $(OEP)Ge(C_6H_5)ClO_4$. In addition, bulk electrolysis of $(OEP)Ge(C_6H_5)_2$ at +1.2 V in PhCN containing 0.1 M TBAP leads to a species that is ESR inactive. Further electrolysis at +1.6 V generates a solution whose ESR signal is detected at low temperature. The spectrum is singlet and symmetrical with a g value of 2.006. This is close to the free spin value, and the absorbance band width of 4.9 G is typical of a porphyrin cation radical which is assigned as $[(OEP)Ge(C_6H_5)ClO_4]^+$. Other $(P)Ge(R)_2$ undergo similar mechanisms.

In conclusion, the photochemistry, electrochemistry, and spectroelectrochemistry of $(P)Ge(R)_2$ are consistent with a mechanism involving cleavage of the germanium–carbon bond. This cleavage is either by irradiation with visible light or by electrooxidation of the complex. The low germanium–carbon bond energy of $(P)Ge(R)_2$ provides the feasibility of generating a very reactive alkyl or aryl radical. Thus, mono-alkyl or aryl monochlorogermanium(IV) porphyrins that cannot be synthesized with standard Grignard reactions are easily formed through photoreactions involving dialkyl or diaryl germanium(IV) porphyrins in $CHCl_3$ or CH_2Cl_2.

Acknowledgment. The support of the National Science Foundation (KMK Grant CHE-8515411 and INT-8413696) and the CNRS are gratefully acknowledged.

Registry No. $(OEP)GeCl_2$, 31713-45-8; $(TPP)GeCl_2$, 41043-38-3; $(OEP)Ge(CH_3)_2$, 110718-62-2; $(OEP)Ge(C_6H_5)_2$, 110718-63-3; $(OEP)Ge(CH_2C_6H_5)_2$, 110718-64-4; $(TPP)Ge(C_6H_5)_2$, 110718-65-5; $(TPP)Ge(CH_2C_6H_5)_2$, 74344-37-9; $(OEP)Ge(C_6H_5)Cl$, 110718-66-6; $(OEP)Ge(C_6H_5)OH$, 110718-67-7; $(OEP)Ge(C_6H_5)ClO_4$, 110718-68-8.

(30) Kadish, K. M.; Xu, Q. Y.; Barbe, J.-M.; Anderson, J. E.; Wang, E.; Guilard, R., submitted to *Inorg. Chem.*

Hydroformylation of Fluoro Olefins, $R_fCH=CH_2$, Catalyzed by Group VIII Transition-Metal Catalysts. Crucial Factors for Extremely High Regioselectivity

Iwao Ojima,*‡ Koji Kato,‡ Masami Okabe,‡ and Takamasa Fuchikami§

Contribution from the Department of Chemistry, State University of New York at Stony Brook, Stony Brook, New York 11794, and Sagami Chemical Research Center, 4-4-1 Nishi-Ohnuma, Sagamihara, Kanagawa 229, Japan. *Received March 31, 1987*

Abstract: Hydroformylations of fluoro olefins, trifluoroprop-1-ene (TFP), pentafluorobut-1-ene (PFB), heptafluoropent-1-ene (HPFP), heptadecafluorodec-1-ene (HPDFD), vinyl fluoride (VF), pentafluorostyrene (PFS), and allylpentafluorobenzene (**4a**), promoted by transition-metal catalysts were studied. Remarkable dependency of the regioselectivity of the reaction on the catalyst metal species (Co, Pt, Ru, and Rh) was found in the reactions of TFP and PFS; e.g., *n*-aldehyde was obtained with >93% selectivity by a cobalt catalyst whereas iso-aldehyde was obtained with >96% selectivity by a rhodium catalyst for the reaction of TFP. On the contrary, the reaction of VF gave 2-fluoropropanal (2-FPA) exclusively, regardless of the metal catalyst species. The effects of temperature and carbon monoxide pressure on the regioselectivity were investigated. Possible mechanisms for the uniquely regioselective hydroformylations are discussed on the basis of the results obtained, and a mechanism that involves an initial formation of isoalkyl–metal species followed by isomerization to *n*-alkyl–metal species and/or followed by carbon monoxide insertion to form isoacyl–metal intermediate was proposed to be the one operating in these reactions.

Hydroformylation of alkenes is an important reaction for the practical synthesis of aldehydes, and detailed studies on the mechanism of the reaction as well as applications to organic syntheses have been extensively studied.[1,2] However, little had been known about the reactions of alkenes bearing perfluoroalkyl or perfluoroaryl substituents when we started the research on this subject.[3] It has been shown that the introduction of trifluoromethyl or fluoro aromatic group into organic compounds often brings about unique chemical and biological properties.[4] Thus, the development of new synthetic methods that enable us to introduce these fluoro groups effectively and selectively to the desired molecules from readily available materials is of significant synthetic importance. With this respect, commercially available fluoro olefins such as 3,3,3-trifluoropropene (TFP), vinyl fluoride (VF), and pentafluorostyrene (PFS) are important starting materials.

Previously we studied the hydroformylation of TFP and PFS as one of our approaches to the functionalizations of these building blocks by means of transition-metal catalysts and briefly reported unusually high regioselectivities and remarkable dependency of the regioselectivities of the reaction on the catalyst metal species, which is very unique in comparison with the hydroformylation of ordinary alkenes.[5,6] We describe here a full account of our

‡State University of New York at Stony Brook.
§Sagami Chemical Research Center.

(1) Pino, P.; Piacenti, F.; Bianchi, M. In *Organic Syntheses via Metal Carbonyls*; Wender, I., Pino, P., Eds.; Wiley-Interscience: New York, 1977; Vol. 2, pp 43–231.

(2) Cornils, B. In *New Syntheses with Carbon Monoxide*; Falbe, J., Ed.; Springer: Berlin, 1980; pp 1–225.

(3) Hydroformylation of hexafluoropropene was reported to give a mixture of hexafluoropropane (50%), alcohols (40%), and aldehydes (5–8%). See: Rudkovskii, D. M.; Imayanitov, N. S.; Gankin, V. Yu. *Tr., Vses. Nauchno-Issled. Inst. Neftekhim. Protsessov* **1960**, 121; *Chem. Abstr.* **1962**, *57*, 10989. A patent claimed the reaction of heptadecafluorodecene, $CF_3(CF_2)_7CH=CH_2$, catalyzed by $Co_2(CO)_8$, which gave the corresponding alcohols or aldehydes. See: Roehrscheid, F. (Hoechst A.G.) *Ger. Offen.* 2 163 752, 1973; *Chem. Abstr.* **1973**, *79*, 78110m.

(4) (a) Filler, R., Ed. *Biochemistry Involving Carbon–Fluorine Bonds*; ACS Symposium Series 28; American Chemical Society: Washington, DC, 1976. (b) Smith, F. A. CHEMTECH **1973**, 422. (c) Filler, R. CHEMTECH **1973**, 752. (d) Filler, R., Kobayashi, Y., Eds.; *Biomedical Aspects of Fluorine Chemistry*; Elsevier Biomedical: Amsterdam, 1982.

(5) Fuchikami, T.; Ojima, I. *J. Am. Chem. Soc.* **1982**, *104*, 3527.

0002-7863/87/1509-7714$01.50/0